23rd ABCM International Congress of Mechanical Engineering
December 6-11, 2015, Rio de Janeiro, RJ, Brazil

NUMERICAL SOLUTION FOR RUBINSTEIN PHASE CHANGE PROBLEM

Bruno dos Reis Jaccoud
Department of Nanotechnology Engineering - COPPE/UFRJ, CP 68501, CT, Federal University of Rio de Janeiro, Rio de Janeiro-RJ, 21941-972, Brazil
bruno.jaccoud@gmail.com

Helcio Rangel Barreto Orlande
Department of Mechanical Engineering – COPPE/UFRJ, CP 68503, CT, Federal University of Rio de Janeiro, Rio de Janeiro-RJ, 21941-972, Brazil
helcio@mecanica.coppe.ufrj.br

Olivier Fudym
CNRS Brasil - Bureau CNRS Brésil, Avenida Presidente Antônio Carlos, 58 /415, Rio de Janeiro-RJ 20020-010, Brazil
olivier.fudym@cnrs-dir.fr

Abdelhalim Benberrah
RAPSODEE - Ecole des Mines d'Albi, Allée des sciences, 81000 Albi, France
abenberr@mines-albi.fr

Aldélio Bueno Caldeira
Department of Mechanical and Materials Engineering, Military Institute of Engineering, Rio de Janeiro - RJ - 22290-270, Brazil
aldelio@ime.eb.br

Abstract. *A model is described for the solidification of an undercooled binary alloy in a one-dimensional semi-infinite medium. The model implemented in this work can be used for cases where the alloy is constituted of nanoparticles dissolved in a base phase change material. The equations of heat and mass transfer are coupled through the interface conditions at the moving phase change boundary. The equations are rewritten in conservative form to implement a numerical technique based on the enthalpy method, which does not require the explicit tracking of the phase change boundary. The obtained results are verified with known analytical solutions and explicit numerical solutions, for a test case available in the literature. The numerical technique used in this work can accurately predict the temperature and the solute concentration for several conditions of practical interest. The effects of the Lewis number on the solidification behavior are examined in the paper as well.*

Keywords: *Binary Alloy, Enthalpy Method, Nanoparticles, Phase Change Materials*

1. INTRODUCTION

The limited supply of energy is one of the difficulties encountered by today's modern society, especially when it comes to the high energy demand from the rapidly growing emerging economies. In response to this challenge, the search for renewable alternative energy has been intensified. However, due to the unpredictable supply of renewable energy sources, storage of all forms of energy is a major obstacle that hinders greater adoption of renewable energy sources. As for the thermal energy storage, considerable amount of energy can be stored at a practically constant temperature, when a material undergoes phase change. Paraffin, water, salt hydrates and sugar alcohols are examples of phase change materials (PCM) with high latent heat storage capacity, with melting temperatures that can be suitable for several practical applications (El Hasadi, *et al.*, 2013).

In this context, as a way of adjusting the time delays associated with power supply and demand, PCM's are considered promising thermal storage materials. The main criterion for selecting a PCM for a given application is its phase change temperature. However, other important parameters should also be taken into account in an appropriate decision (El Hasadi, *et al.*, 2013; Dhaidan, *et al.*, 2013).

Many research groups have contributed to this area by studying analytically (Fan and Khodadadi, 2011; El Hasadi, 2013), numerically (Khodadadi and Hosseinizadeh, 2007; Hosseinizadeh *et al*, 2012; Ranjbar *et al.*, 2011; Kashani *et al.*, 2012) and experimentally (Cui *et al.*, 2011; Sanusi *et al.*, 2011) phase change problems in binary alloys. Experimental methods play important roles in investigating the solidification process. Mathematical numerical modeling has been and continues to be a powerful tool in improving the understanding of the solidification process.

Numerical problems involving solidification, which exhibit a moving and sharp interface between the solid and liquid phases, are computationally challenging. The requirement to accurately track the solid-liquid interface as it

moves over the discretized domain is the main difficulty in this case. Many popular numerical solutions used to overcome this difficulty are based on enthalpy formulation (Crank, 1984; Voller, 2006). Based on a governing equation that conserves the energy (enthalpy), this method has been used since the middle of last century (Eyres, *et al*, 1946;. Price and Slack, 1954). This equation is valid throughout the problem domain and can be numerically solved, at each step, on a fixed space grid. From the calculated nodal enthalpy field an auxiliary variable –the liquid fraction ($f=1$ in liquid, $f=0$ in solid) - can be extracted and used to track the movement of the solid-liquid interface (Price and Slack, 1954; Voller and Cross, 1981; Date, 1992). Enthalpy methods have been widely verified against alternative approaches to track solidification fronts.

The objective of this work is to explore enthalpy methods to solve binary-alloy one-dimensional phase-change problems, in the presence of an undercooled liquid by using an implicit scheme, for fast and accurate solutions. During solidification, colloidal suspensions behave similarly to a binary alloy when the particle sizes are small. Furthermore, another aspect of the process is the undercooling resulting in rejection of the nanoparticles ahead of the solid-liquid interface (Peppin, *et al*.,2006). In fact, a full analysis of solidification nanostructure-enhanced phase change materials (NePCM) colloidal suspensions must account for mass transfer of the particles (El Hasadi, *et al*., 2013).

Voller (2006; 2008), Alexiades and Solomon (1984) and Wilson et al. (1984) highlighted an important shortcoming of Crowley and Ockendon (1979) enthalpy solution. In fact, the solute rejected into the liquid as the solid is formed is not easily removed from the region ahead of the solid–liquid interface when the Lewis number is large. According to Kurs, *et al*. (1986) this situation can lead to the so-called constitutional under-cooling, in which there is a region ahead of the interface where the equilibrium temperature, calculated by substituting the solute concentration into the liquidus line of the phase diagram, is above the real temperature, see Fig. 1. In a physical context, any small solid imperfection forming on the interface will find itself in a local environment favorable for further growth, resulting in a break down of the solid–liquid interface into a mushy region, where, at the scale of the problem, distinct solid and liquid regions cannot be identified (Voller, 2008).

In this work, we apply the implicit enthalpy method, as an extension of the explicit enthalpy method proposed by Voller (2008), in order to solve the growth of equiaxed dendritic crystals in initially under-cooled melts reported by Crowley and Ockendon (1979).

The proposed solution method is verified with Stefan's problem for the solidification of a binary alloy in a semi-infinite geometry cooled from one side, which is the well-known Rubinstein problem (Rubinstein, 1971). We also verify the present solution for Rubinstein problem with undercooling by using the work of Voller (2008). The present numerical solution will be used in the future for the solution of inverse problems related to the thermal energy storage in phase change materials.

2. MATHEMATICAL MODEL

2.1 Parameters and variables

The non-dimensional parameters used in the current study are as follows:

$$H=\frac{H^*}{L_n^*},\quad T=\frac{T^*-T_m^*-m_L C_0}{L_n^*/c_{npL}^*},\quad C=\frac{C^+}{C_0},\quad x=\frac{x^*}{l},\qquad s=\frac{s^*}{l},\quad t=\frac{\alpha_{nL}t^*}{l^2},$$
$$\alpha=\frac{\alpha_{nS}^*}{\alpha_{nL}^*},\quad D=\frac{D_{nS}^*}{D_{nL}^*},\quad c_p=\frac{c_{npS}^*}{c_{npL}^*},\quad k=\frac{m_L}{m_S},\quad Le=\frac{\alpha_{nL}^*}{D_{nL}^*},\quad St=m_L C_0\frac{c_{npL}^*}{L_n^*},\quad T_{equ}=-St(1-C_L) \tag{1}$$

The superscript * represents dimensional quantities. Subscripts n, S and L identify colloidal mixture, solid and liquid phases, respectively. H^* is enthalpy [J/m^3], H is the dimensionless enthalpy , T^* is the temperature [K], T is the dimensionless temperature, T_m^* is the melting temperature of the pure PCM or solvent [K], l is an appropriate length scale [m], L_n^* is the volumetric latent heat [J/m^3], c_p^* is the volumetric specific heat [J/m^{3}K], c_p is the normalized specific heat, C^+ is solute concentration [wt%], C_0 is the initial volume concentration [wt%], C is the concentration normalized by C_0, s is the location of the solid–liquid interface, t is time, α^* is the thermal diffusivity [m^2/s], D^* is mass diffusivity [m^2/s], D is the normalized mass diffusivity of the nanoparticles, k is the segregation coefficient. The temperature at $x=0$ (i.e., T_{sur}) was lowered below the initial liquidus temperature to initiate the solidification process and for the solid–liquid interface to move away from the cold surface. Other variables of interest are m [K], which is the slope of the assumed straight liquidus (L) or solidus lines (S) in the phase diagram

(see Fig.2), Le is the Lewis number, St is the solutal Stefan number, and T_{equ} is the dimensionless equilibrium temperature of the liquidus line in the phase diagram.

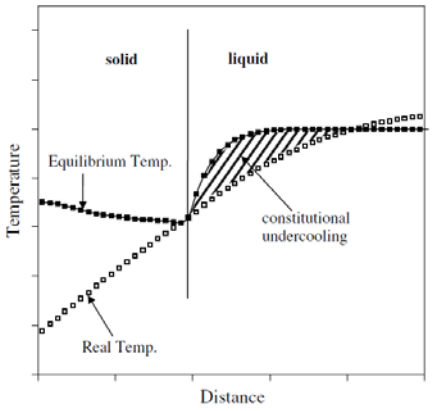

Figure 1. Region of constitutional under-cooling (Voller, 2008).

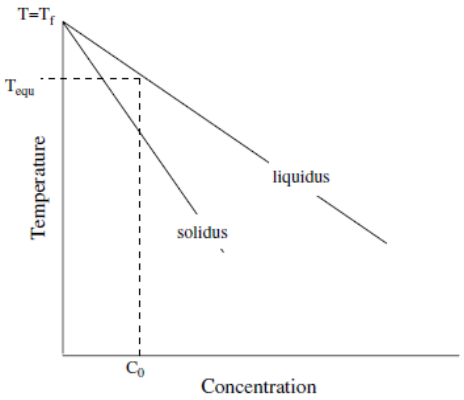

Figure 2. Schematic of binary phase diagram

2.2 Governing equations

The problem under analysis involves a binary alloy melt at a uniform solute concentration C_L and uniform temperature T_0 held in a one-dimensional semi-infinite domain, $x > 0$. At time $t = 0$ the temperature of the surface of this domain is fixed to a temperature T_{sur} sufficient to initiate solidification, so that, as time increases, a solid layer $x = s(t)$ grows from the $x = 0$ surface into the liquid alloy. Following Alexiades and Solomon (1984), the governing equations are given below.

Energy equation and solute diffusion in the solid region:

$$\frac{\partial T_S}{\partial t} = \alpha \frac{\partial^2 T_S}{\partial x^2}, \qquad \frac{\partial C_S}{\partial t} = \frac{D}{Le}\frac{\partial^2 C_S}{\partial x^2}, \qquad 0 < x < s(t) \tag{2}$$

Energy equation and solute diffusion in the liquid melt region:

$$\frac{\partial T_L}{\partial t} = \frac{\partial^2 T_L}{\partial x^2}, \qquad \frac{\partial C_L}{\partial t} = \frac{1}{Le}\frac{\partial^2 C_L}{\partial x^2}, \qquad x > s(t) \tag{3}$$

The initial non-dimensional conditions and the boundary conditions of the PCM are the following:

$$T = T_0, \qquad C = 1 \quad \text{at} \quad t = 0 \quad \text{in} \quad x > 0 \tag{4}$$

$$\frac{\partial C_S}{\partial x} = 0, \quad T = T_{sur} \quad \text{at} \quad x = 0, \quad t > 0 \tag{5}$$

$$C_L = 1, \quad T = T_0 \quad \text{as} \quad x \to \infty, \quad t > 0 \tag{6}$$

On the moving solid–liquid interface $x = s(t)$ there is, due to the partitioning of the solute, a jump in solute concentration, such as shown in Fig. 2 in the binary phase diagram, so that:

$$C_S(s,t) = kC_L(s,t) = kC^i(t) \quad \text{at} \quad x = s(t), \quad t > 0 \tag{7}$$

where $C^i(t)$ is the liquid concentration on the interface. In addition, the temperature of the interface is given by the liquidus line, i.e.

$$C^i(t) = T_{equ}(s,t) = -St(1-C^i(t)) \quad \text{at} \quad x = s(t), \quad t > 0 \tag{8}$$

Further, by neglecting flow due to density changes, the heat balance (Stefan condition) and mass balance on the moving solid–liquid interface at $x = s(t)$ are written as

$$c_p \alpha \left.\frac{\partial T}{\partial x}\right|_{S^-} - \left.\frac{\partial T}{\partial x}\right|_{S^+} = \frac{ds}{dt} \quad \text{at} \quad x = s(t), \quad t > 0 \tag{9}$$

$$\frac{D}{Le}\frac{\partial C_S}{\partial x} - \frac{1}{Le}\frac{\partial C_L}{\partial x} = (1-k)C_i\frac{ds}{dt} \quad \text{at} \quad x = s(t), \quad t > 0 \tag{10}$$

2.3 Similarity solution

The location of the moving interface can be calculated from the following relation (Rubinstein, 1971):

$$s = 2\lambda\sqrt{(t)} \tag{11}$$

and the temperature and concentration profiles are given by (Rubinstein, 1971)

$$T = T_{sur} + (T^i - T_{sur})\frac{\operatorname{erf}\left(\frac{1}{\sqrt{\alpha}}\frac{\mathrm{x}}{2\sqrt{\mathrm{t}}}\right)}{\operatorname{erf}\left(\frac{\lambda}{\sqrt{\alpha}}\right)}, \quad 0 < x < s(t), \quad t > 0 \tag{12}$$

$$C_S = kC^i, \quad 0 < x < s(t), \quad t > 0 \tag{13}$$

$$T = T_0 + (T^i - T_0)\frac{\operatorname{erfc}\left(\frac{\mathrm{x}}{2\sqrt{\mathrm{t}}}\right)}{\operatorname{erfc}(\lambda)}, \quad x > s(t), \quad t > 0 \tag{14}$$

$$C_L = 1 + (C^i - 1)\frac{erfc\left(\frac{x\sqrt{Le}}{2\sqrt{t}}\right)}{erfc\left(\lambda\sqrt{Le}\right)}, \quad x > s(t), \quad t > 0 \tag{15}$$

satisfy the heat and mass transport governing Eqs. (2)-(3) along with the initial and boundary conditions. The three unknowns in these equations, C^i, T^i and λ, leading to a closed solution, are obtained by satisfying the condition set by the liquidus slope

$$T^i + St(1-C^i) = 0 \tag{16}$$

and the heat (9) and mass (10) balance conditions on the moving interface $x = s(t)$ given respectively by

$$\sqrt{\pi}\lambda - c_p\sqrt{\alpha}\,\frac{T^i - T_{sur}}{\operatorname{erf}\left(\dfrac{\lambda}{\sqrt{\alpha}}\right)}\mathrm{e}^{\frac{\lambda^2}{\alpha}} - \frac{T^i - T_0}{\operatorname{erfc}(\lambda)}\mathrm{e}^{-\lambda^2} = 0 \tag{17}$$

$$(1-k)C^i\lambda\sqrt{Le}\sqrt{\pi}e^{\lambda^2 Le}\operatorname{erfc}(\lambda\sqrt{Le}) - (C^i - 1) = 0 \tag{18}$$

3. ENTHALPY MODEL FOR THE BINARY-ALLOY SOLIDIFICATION

For the binary-alloy problems the enthalpy model is developed from the model presented by Crowley and Okendon (1979). Enthalpy, *H*, is defined as the sum of sensible and latent heats. The chemical activity and the concentration play the same roles in the mass transfer problem as the temperature and enthalpy in the heat-transfer problem. Eqs. (2)-(3) may now be written as

$$\begin{aligned}\frac{\partial H}{\partial t} &= \nabla\left(\alpha^{\mathrm{f}}\nabla T\right), \qquad x > 0\\ \frac{\partial C^{\mathrm{f}}}{\partial t} &= \nabla\left(D^{\mathrm{f}}\nabla V\right), \qquad x > 0\end{aligned} \tag{19}$$

where the additional mixture definitions are $\alpha^{\mathrm{f}} = f + (1-f)c_p\alpha$ and $D^{\mathrm{f}} = {}^{1}\!/_{Le}[f + k(1-f)D]$ (Crowley and Ockendon, 1979). Note that when $f = 0$ the solid phase transport Eqs. (2) are recovered from (19) and when $f = 1$ the liquid phase equations (3) and (19) are recovered. Crowley and Ockendon (1979) observed that Eq. (19) is the solute equivalent of the enthalpy equation ; C^f, taking the role of enthalpy, jumps across the solid–liquid interface and, *V*, taking the role of temperature, is piecewise continuous across the interface.

According to Voller (2008) in a treatment which allows for problems that involve different specific heat values in the solid and liquid phases we have

$$H = \begin{cases} T + 1 & \text{if} \quad f = 1 \\ T_{equ} + f & \text{if} \quad 0 < f < 1 \\ T_{equ} + c_p(T - T_{equ}) & \text{if} \quad f = 0 \end{cases} \tag{20}$$

Where $0 \le f \le 1$ is the liquid fraction so that the mixture solute concentration is defined by

$$C^f = fC_L + (1-k)C_S \tag{21}$$

and – following the initial idea of Crowley and Ockendon (1979) – a concentration potential is defined as

$$V = \frac{C^f}{f + (1-k) + k} \tag{22}$$

4. NUMERICAL SOLUTION OF ENTHALPY FORMULATION

In the following, a numerical solution is developed for Eqs. (19) - (22), by using an implicit scheme.

4.1 The finite volume equations

A numerical solution is developed below for Eqs. (19) in a one-dimensional solidification of a block of molten alloy, with uniform initial temperature and concentration, T_0 and C_0^f, respectively. At the initial time, the temperature at the surface $x = 0$ is lowered to T_{sur}, where it is assumed a zero mass flux boundary condition. The Eq. (19) is solved to update the nodal enthalpy and mixture concentration fields.

The implicit schemes of (19) is

$$H_i^{n+1} = H_i^n + \frac{\Delta t}{\Delta x^2} K_w (T_{i-1}^{n+1} - T_i^{n+1}) + K_e (T_{i+1}^{n+1} - T_i^{n+1})$$
$$C_i^{f-n+1} = C_i^{f-n} + \frac{\Delta t}{\Delta x^2} D_w (V_{i-1}^{n+1} - V_i^{n+1}) + D_e (V_{i+1}^{n+1} - V_i^{n+1}) \quad (23)$$

where Δt is the time step, Δx is the space step, and the lower case subscripts w(est) and e(ast) indicate the face values for the control volume with center node *i*. The values of the interface conductivities and diffusivities are calculated as $K_w = \left[\frac{2(f_{j-1} f_i)}{f_{j-1} + f_i} + \left(1 - \frac{2(f_{j-1} f_i)}{f_{j-1} + f_i} \right) \alpha \right]$ and $D_w = \frac{1}{Le} \left[\frac{2(f_{j-1} f_i)}{f_{j-1} + f_i} + k \left(1 - \frac{2(f_{j-1} f_i)}{f_{j-1} + f_i} \right) D \right]$.

The resulting fields are then used in a point by point iteration to extract the nodal values of V, T and f that are needed in the next time step. The spatial domain is discretized with 1000 control volumes of length $\Delta x = 0.05$, and a time step of $\Delta t = 25 \times 10^{-5}$. The choice of space step is sufficient to satisfy grid independence and the choice of time steps is sufficient to avoid stability problems.

5. RESULTS

At the start of the calculation all node values are set to $f_i = 1, C_i^f = 1;\ T_i = T_0;\ V_i = 1$ and $H_i = T_i + 1$. In order to initiate solidification at volume $i = 1$ we set $f_1 = 0.999$ at this control volume. Calculations are carried out until the solid-liquid interface reaches $s = 9.75$. Calculations are made for the binary-alloy problem defined by the properties (Voller, 2008)

$$T_{sur} = -1, \quad T_0 = 0.1, \quad \alpha = 1.5, \quad c_p = 2, \quad k = 0.1, \quad Le = 4.0, \quad D = Le, \quad St = -0.1 \quad (24)$$

In this paper since the solute concentration in the solid phase will take a fixed constant value, the choice of solid mass diffusivity has no influence. As such, the setting of $D = Le$ was made to ensure that stability of the discrete solute transport equation is met as the Lewis number is increased.

Figure 3 compares predictions from the analytical Rubinstein solution with the implicit and explicit enthalpy solution for the case where constitutional under-cooling occurs. This figure shows results for (a) the interface, (b) the concentration history for the 90th node point, at $x = 4.475$, and (c) the temperature history at $x = 4.475$. In all plots the numerical results are shown as symbols and the analytical results as continuous lines. In all cases the agreement between the numerical and analytical results is excellent at the graphic scale.

The use of an implicit solution was devoted to remove the inherent instability of explicit solutions. It is clear in figures 3 that the fidelity between the analytical and numerical solutions is retained in all predicted fields. The prediction of the equilibrium temperature in the solid indicates that, for the choice of boundary condition at $x = 0$, the predicted concentration at which the phase change occur remains fixed throughout the solidification. It is stressed that this condition occurs naturally in both the analytical and numerical solutions, i.e., it is not imposed or assumed a priori.

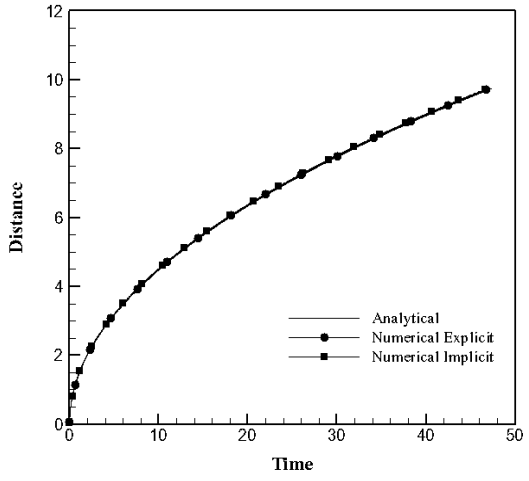

(a)

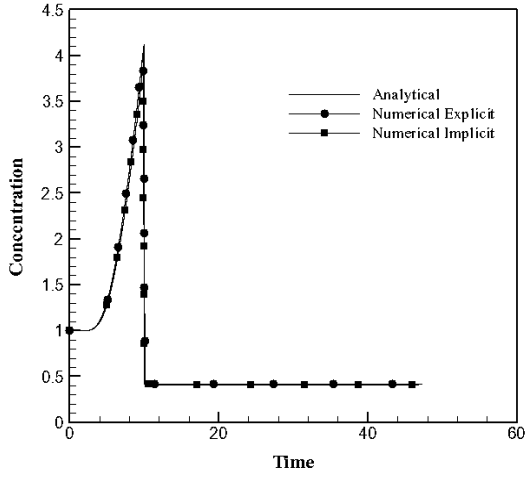

(b)

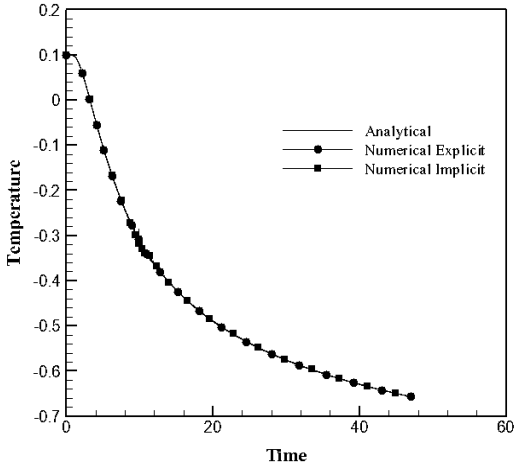

(c)

Figure 3. Results for compositional under-cooling case, symbols are numeric results lines are analytical. (a) Interface movement, (b) concentration history at x=4.475, (d) temperature history at x=4.475.

The Lewis number characterizes the relative roles of the thermal and solute diffusion in controlling the solid–liquid interface movement. An increase in the Lewis number leads to a relative decrease in the width of the solute boundary layer ahead of the solidification front. Figures 4 show the solute and temperature profiles at dimensionless time $t = 40$ for case where $Le = 1$, 0.1 and 1 (figures from left to right). As expected, the thermal and solutal boundary layers have approximately the same thicknesses for $Le = 1$. With the increase of the Lewis number the rate of solute diffusion is reduced, the interface solute pile up increases and the solutal boundary layer is thinner than the thermal boundary layer. On the other hand, if the Lewis number is decreased, the rate of the solute diffusion away from the interface increases, the pile up of solute at the solid–liquid interface is reduced, and the solutal boundary layer becomes thicker than the thermal boundary layer.

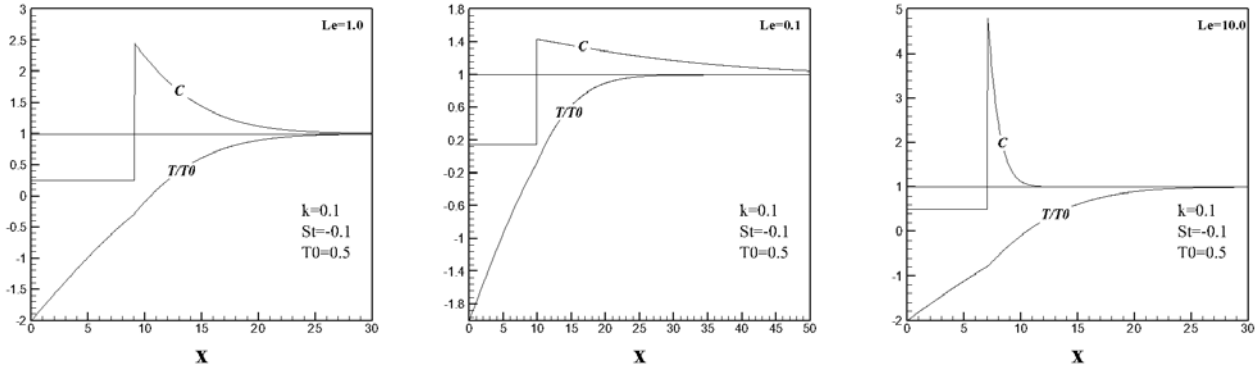

Figure 4. Concentration and temperature profiles at time t = 40 for Lewis numbers of 1, 0.1 and 10, respectively

6. CONCLUSIONS

This paper presents a numerical solution for the solidification of an under-cooled binary alloy melt. Solidification was initiated by introducing, at the cool surface, a solid fraction at the equilibrium temperature. The similarity solution proposed by Rubinstei (1971) provides important quantitative insights into the relative roles of thermal and solute diffusive transport during solidification, and identifies physical limits that will allow for growth from a solid seed.

An implicit enthalpy numerical solution was developed, based previously on the enthalpy binary-alloy model proposed by Crowley and Okendon (1979). The performance of the implicit enthalpy method is verified with the

available analytical and explicit solutions of Voller (2008). The agreement between the implicit solution developed in this work and such benchmark solutions is excellent.

7. ACKNOWLEDGEMENTS

This work was partially funded by CAPES (agency for the fostering of science from the Brazilian Ministry of Science and Education).

8. REFERENCES

Alexiades, V. and Solomon, A.D., 1984. "Mathematical Modeling of Melting and Freezing Processes", Hemisphere, Washington, pp. 106–109.

Crank, J., 1984. "Free and Moving Boundary Problems", Claendon Press, Oxford.

Crowley, A.B. and Ockendon, J.R., 1979. "On the numerical solution of an alloy solidification problem", Int. J. Heat Mass Transfer, Vol. 22, pp. 941–947.

Cui, Y., Liu, C., Hu, S., Yu, X., 2011. "The experimental exploration of carbon nanofiber and carbon nanotube additives on thermal behavior of phase change materials", Sol. Energy Mater. Sol. Cells., Vol. 95, pp. 1208–1212.

Date, A.W., 1992. "Novel strongly implicit formulation for multidimensional Stefan problems", Numer. Heat Transfer B, Vol. 27, pp. 231–251.

Dhaidan, N.S., Khodadadi, J.M., Al-Hattab, T.A., Al-Mashat, S.M., 2013. "Experimental and numerical investigation of melting of NePCM inside an annular container under a constant heat flux including the effect of eccentricity", Int. J. Heat Mass Transfer, Vol. 66, pp. 672-683.

El Hasadi, Y.M.F., Khodadadi, J.M. 2013. "One-dimensional Stefan problem formulation for solidification of nanostructure-enhanced phase change materials (NePCM)", Int. J. Heat Mass Transfer, Vol. 67, pp. 202-213.

Eyres, N.R., Hartree, D.R., Ingham, J., Jackson, R., Sarjant, R.J., Wagstaff, S.M., 1946. "The calculation of variable heat flow in solids", Phil. Trans. R. Soc. A, Vol. 240, pp. 1–57.

Fan, L., Khodadadi, J.M., 2011. "Thermal conductivity enhancement of phase change materials for thermal energy storage: a review", Renewable Sustainable Energy Rev., Vol. 15, pp. 24–46.

Hosseinizadeh, S.F., Darzi, A.R., Tan, F., 2012, "Numerical investigations of unconstrained melting of nano-enhanced phase change material (NEPCM) inside a spherical container", Int. J. Therm. Sci., Vol. 51, pp. 77–83.

Kashani, S., Ranjbar, A.A., Abdollahzadeh, M., Sebti, S., 2012. "Solidification of nanoenhanced phase change material (NEPCM) in a wavy cavity", Heat Mass Transfer, Vol. 48, pp. 1155–1166.

Khodadadi, J.M., Hosseinizadeh, S.F., 2007 "Nanoparticle-enhanced phase change materials (NEPCM) with great potential for improved thermal energy storage", Int. Commun. Heat Mass Transfer, Vol. 34, pp. 534–543.

Kurz, W. and Fisher, D.J., 1986. "Fundamentals of Solidification", Trans Tech Publishing, Switzerlan, pp. 53–54.

Peppin, S.S.L., Elliott, J.A.W., Worster, M.G., 2006. "Solidification of colloidal suspensions", J. Fluid Mech., Vol. 554, pp. 147–166.

Price, P.H. and Slack, M.R., 1954. "The effect of latent heat on numerical solutions of the heat flow equation", Br. J. Appl. Phys., Vol. 5, pp. 285-287.

Ranjbar, A.A., Kashani, S., Hosseinizadeh, S.F., Ghanbarpour, M., 2011. "Numerical heat transfer studies of a latent heat storage system containing nano-enhanced phase change material", Therm. Sci., Vol. 15, pp. 169–181.

Rubinstein, L., 1971. "The Stefan Problem, Translations of Math", Monographs, Vol. 27, American Mathematical Society, Providence.

Sanusi, O., Warzoha, R. Fleischer, A.S., 2011. "Energy storage and solidification of paraffin phase change material embedded with graphite nanofibers", Int. J. Heat Mass Transfer, Vol. 54, pp. 4429–4436.

Voller, V.R. and Cross, M., 1981. "Accurate solutions of moving boundary problems using the enthalpy method", Int. J. Heat Mass Transfer, Vol. 24, pp. 545–556.

Voller, V.R., 2006. "Numerical methods for phase-change problems", in: W.J. Minkowycz, E.M. Sparrow, J.Y. Murthy (Eds.), Handbook of Numerical Heat Transfer, John Wiley, New York, pp. 593–622.

Voller, V.R., 2008. "A numerical method for the Rubinstein binary-alloy problem in the presence of an under-cooled liquid", Int. J. Heat Mass Transfer, Vol. 51, pp. 696-706.

Wilson, D.G., Solomon, A.D., Alexiades, V., 1984. "A model of binary alloy solidification", Int. J. Numer. Meth. Eng., Vol. 20, pp.1084–1967.

9. RESPONSIBILITY NOTICE

The authors are the only responsible for the printed material included in this paper.